molecules

MDPI

Article

The CO_2 Absorption in Flue Gas Using Mixed Ionic Liquids

Guoqing Wu, Ying Liu *, Guangliang Liu and Xiaoying Pang

College of Chemistry and Chemical Engineering, Inner Mongolia University, Hohhot 010021, China; 15771380268@163.com (G.W.); 111975317@imu.edu.cn (G.L.); Pmmwhydedabai@163.com (X.P.)

* Correspondence: celiuy@imu.edu.cn; Tel.: +86-471-4992981

Academic Editors: Monica Nardi, Antonio Procopio and Maria Luisa Di Gioia

Received: 22 January 2020; Accepted: 22 February 2020; Published: 25 February 2020

Abstract: Because of the appealing properties, ionic liquids (ILs) are believed to be promising alternatives for the CO_2 absorption in the flue gas. Several ILs, such as [NH_2emim][BF_4], [C_4mim][OAc], and [NH_2emim[OAc], have been used to capture CO_2 of the simulated flue gas in this work. The structural changes of the ILs before and after absorption were also investigated by quantum chemical methods, FTIR, and NMR technologies. However, the experimental results and theoretical calculation showed that the flue gas component SO_2 would significantly weaken the CO_2 absorption performance of the ILs. SO_2 was more likely to react with the active sites of the ILs than CO_2. To improve the absorption capacity, the ionic liquid (IL) mixture [C_4mim][OAc]/[NH_2emim][BF_4] were employed for the CO_2 absorption of the flue gas. It is found that the CO_2 absorption capacity would be increased by about 25%, even in the presence of SO_2. The calculation results suggested that CO_2 could not compete with SO_2 for reacting with the IL during the absorption process. Nevertheless, SO_2 might be first captured by the [NH_2emim][BF_4] of the IL mixture, and then the [C_4mim][OAc] ionic liquid could absorb more CO_2 without the interference of SO_2.

Keywords: flue gas; carbon dioxide; absorption; ionic liquids

1. Introduction

The CO_2 absorption of flue gas is an important process for reducing greenhouse gas [1]. To date, most flue absorptions are performed by using amine solvents. However, conventional absorption methods usually have some disadvantages: High equipment corrosion rate, high absorbent make-up rate due to the amine degradation by SO_2, NO_2, and O_2 in the flue gas, and high energy consumption during the regeneration process [2]. In the last decades, ionic liquids (ILs) have been used in many fields. Multifunctional ionic liquids are easily prepared, and the vapor pressure of ionic liquids can be neglected [3]. The other attractive properties of ILs include: High thermal stability, large electrochemical window, and high dissolve ability of compounds [4]. Blanchard et al. [5] have reported that certain ILs can considerably dissolve CO_2 gas. Since then, ILs for CO_2 capture have attracted much attention. For example, multi-*N*-containing ionic liquids can absorb much more SO_2/CO_2 in the flue gas than that of the limestone solvent [6]. Shiflett et al. [7,8] have found that the imidazolium-based ionic liquid [C_4mim][OAc] can markedly reduce the energy losses of CO_2 absorption comparing with those of the commercial monoethanolamine solvent. Guanidinium salt ILs (e.g., [TMG][L]) and functional ILs (e.g., [NH_2p-bmim][BF_4] and 2-(2-hydroxyethoxy) ammonium acetate) all show high efficiency for CO_2 and SO_2 capture [9,10].

The typical flue gas from coal-burning usually contains about 15 vol% CO_2, 10 vol% H_2O, and more than 2 vol% SO_2 [11]. Apart from CO_2, the effects of SO_2 on the flue gas absorption should be taken into account [12]. Most researchers consider that water has a little influence on the CO_2 capture, but the effects of SO_2 would not be neglected. For the impurities of the flue gas, it is found

that the ILs are more likely to absorb SO_2 than CO_2. Specifically, the N element of the ionic liquid (IL) prefers to capture the SO_2 molecules, and then CO_2 molecules are repelled by the captured SO_2 [13]. Thus, the CO_2 absorption capacity of ionic liquids would be rapidly decreased over several cycles. Moreover, almost all of the ILs would exhibit much higher SO_2 absorption capacity than CO_2 due to the higher solubility of SO_2 in ILs. For instance, pure CO_2 solubility in the guanidinium-based ILs was only 0.4 mol/mol, while the SO_2 solubility in these ILs was as high as 2.5 mol/mol under the same conditions [10]. For an extreme case, the absorption capacities of pure SO_2 and CO_2 in the azole-based ILs (e.g., [P_{66614}][Im]) were 3.5 mol/mol and 0.1 mol/mol, respectively [14]. Although SO_2 has stronger interactions with ILs than CO_2 does, the actual partial pressure of SO_2 in the flue gas is very low [15]. It is well accepted that the partial pressure of SO_2 is about two orders of magnitude lower than that of CO_2, and low SO_2 partial pressure usually leads to low absorption capacity for SO_2. That is, a lot of energy will be consumed to remove SO_2 and CO_2 from the flue gas, if we used a two-step absorption process (absorbing SO_2 at first, and then CO_2).

The effects of single IL on the CO_2 capture have been widely discussed in recent years [2,7,16–19]. However, there are few reports on the IL mixtures for CO_2 absorption, especially on the CO_2 capture from the flue gas. Therefore, if the IL mixture was employed, the CO_2 absorption capacity of the mixed ILs might be greater than that of the single ionic liquid. Specifically, if the SO_2 of flue gas was absorbed by one IL of the mixture, the negative influence of SO_2 on the whole IL mixture might be significantly decreased, and then more CO_2 could be captured.

In this work, we want to use IL mixtures to remove CO_2 and SO_2 from the flue gas. The amine-functional ionic liquid [NH_2emim][BF_4] and the imidazolium-based ionic liquid [C_4mim][OAc] were synthesized at first. Subsequently, the two ILs were mixed to investigate the CO_2 and SO_2 absorption. Here, [NH_2emim][BF_4] was mainly used to absorb SO_2 in the flue gas, while the [C_4mim][OAc] ionic liquid was employed to capture CO_2. In order to more clearly study the actual flue gas, the CO_2 absorption performance in the IL mixture was measured at the simulated flue gas with 15 vol% CO_2 and 2 vol% SO_2. The effect of SO_2 on the IL mixture and the interaction between CO_2 and SO_2 in the IL absorption were also studied. Furthermore, the absorption mechanism at the molecule level was investigated by the quantum chemical calculation and the instrumental analysis.

2. Results and Discussion

2.1. CO_2 and SO_2 Absorption Performance of the Single ILs

When the simulated flue gas (15% CO_2/85% N_2) only contains the CO_2 impurity, one mole [C_4mim][OAc] could absorb 0.298 mol CO_2 (Table 1). However, when SO_2 was mixed in the simulated flue gas (15% CO_2/2% SO_2/N_2), the CO_2 absorption capacity of [C_4mim][OAc] was reduced to 0.204 CO_2/mol IL. The result shows that SO_2 has a negative effect on the IL absorbing CO_2. The single IL [NH_2emim][OAc] and [NH_2emim][BF_4] were also used to capture the CO_2 of flue gas. Without the interference of SO_2, the CO_2 absorption capacities of [NH_2emim][OAc] and [NH_2emim][BF_4] were 0.291 mol CO_2/mol IL and 0.290 mol CO_2/mol IL, respectively. However, like the [C_4mim][OAc] ionic liquid, the CO_2 absorption capacities under exposure to 2% SO_2 would be markedly decreased to 0.171 mol CO_2/mol [NH_2emim][OAc] and 0.180 mol CO_2/mol [NH_2emim][BF_4], respectively. In short, the single ionic liquids all exhibit the CO_2 absorption capacities, but this capacity would be greatly weakened by the interference of SO_2.

Table 1. Summary of CO_2 absorption capacity by single ionic liquids.

Ionic Liquids	T, *K*	Gas	Absorption Capacity, mol CO_2/mol IL
[C_4mim][OAc]	293	15% CO_2/85% N_2	0.298
[C_4mim][OAc]	293	15% CO_2/2% SO_2/83% N_2	0.204
[NH_2emim][BF_4]	293	15% CO_2/85% N_2	0.290
[NH_2emim][BF_4]	293	15% CO_2/2% SO_2/83% N_2	0.180
[NH_2emim][OAc]	293	15% CO_2/85% N_2	0.291
[NH_2emim][OAc]	293	15% CO_2/2% SO_2/83% N_2	0.171

The researchers believed that CO_2 and SO_2 of the flue gas would be absorbed simultaneously [13,20]. The [C_4mim][OAc] and [NH_2emim][BF_4] absorption results supported this conclusion. For example, an experiment was carried out of outlet SO_2 concentration vs. time to investigate the SO_2 absorption performance. In this study (Figure 1a), the simulated flue gas contained 15% CO_2, 2% SO_2, and 83% N_2. The concentrations of CO_2 and SO_2 of the outlet stream were simultaneously detected with time. It was found that [C_4mim][OAc] and [NH_2emim][BF_4] all can capture CO_2, but the outlet SO_2 concentration was hardly detected before 40 min (Figure 1a). It indicates that SO_2 could be completely absorbed by [C_4mim][OAc] and [NH_2emim][BF_4] during the absorption process. Additionally, an extreme case was investigated in which the simulated flue gas contained 80% CO_2, 2% SO_2, and 18% N_2. However, SO_2 was also not found at the gas stream of the outlet before 15 min. Compared with CO_2, SO_2 has higher dipole moments and molecular polarity, which often results in the strong affinity of SO_2 with ionic liquids [21,22].

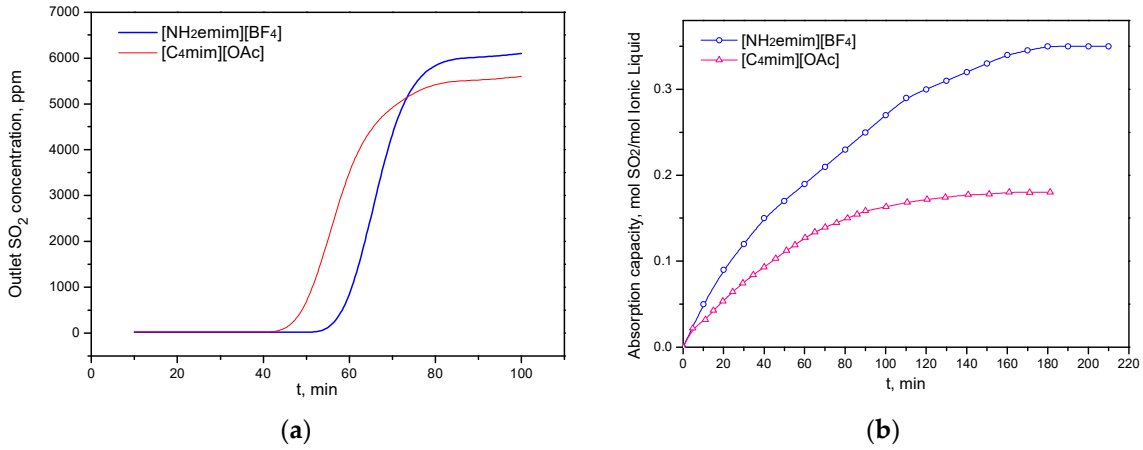

Figure 1. SO_2 absorption performance of [C_4mim][OAc] and [NH_2emim][BF_4]: (**a**) Outlet SO_2 concentration vs. time at the atmosphere of 15% CO_2, 2% SO_2, and 83% N_2; (**b**) SO_2 absorption capacity at the atmosphere of 2% SO_2/98% N_2.

The presence of SO_2 in flue gas usually leads to a competitive and negative influence on the separation of CO_2. Figure 2 shows the CO_2 absorption performance of [C_4mim][OAc] at the atmosphere of 15% CO_2/85% N_2 and 15% CO_2/2% SO_2/83% N_2, respectively. After 6 regeneration cycles, 1 mol [C_4mim][OAc] could absorb 0.255 mol CO_2, although the IL absorption capacity slightly decreased. In contrast, the absorption capacity of 1 mol [C_4mim][OAc] was only 0.10 mol CO_2 after the same number of cycles. In addition, the net SO_2 absorption experiment (2% SO_2/98% N_2) showed that [NH_2emim][BF_4] has high SO_2 absorption capacity (0.35 mol SO_2/mol IL), while 1 mol [C_4mim][OAc] only absorbs 0.18 mol SO_2 (Figure 1b). These results agreed well with previous studies [23–25].

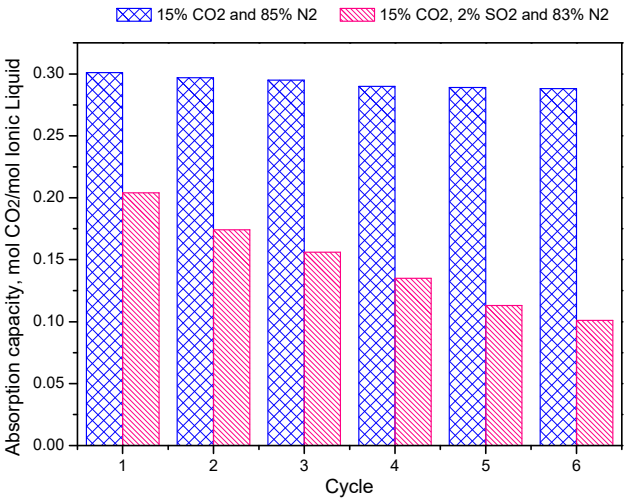

Figure 2. CO_2 absorption capacity of [C_4mim][OAc] during 6 regeneration cycles at the atmosphere of 15% CO_2/85% N_2 and 15% CO_2/2% SO_2/83% N_2.

FT-IR can investigate the interaction between IL and CO_2/SO_2 [26]. The spectra of [C_4mim][OAc] showed the changes after 15% CO_2 and 2% SO_2 absorption, respectively (Figure 3a–c). However, the [C_4mim][OAc] spectrum had minimal changes when it was used to remove pure CO_2. Although the appearance of the carbonyl band at 1720 cm^{-1} shows that the acetate anion might be partly converted into the acetate acid [27], Shiflett considered that the amount of such a chemical reaction was minor and reversible [24]. Thus, the other reactions between CO_2 and the cation species in this work might not be detected within the wavenumber of 800–1600 cm^{-1}, as Figure 3a,c shown. Similarly, the FT-IR spectra of [NH_2emim][BF_4] almost have no change before and after CO_2 absorption (Figure 3d,f), indicating that the chemical reaction between the [NH_2emim] cation and CO_2 was not enough to be detected by FT-IR.

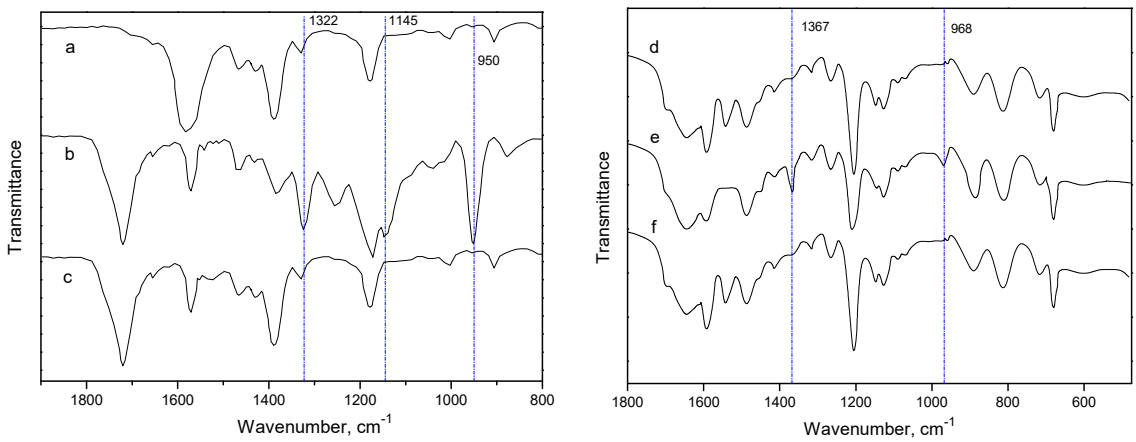

Figure 3. FT-IR spectra of ionic liquids (ILs): (**a**) Fresh [C_4mim][OAc]; (**b**) [C_4mim][OAc] after SO_2 absorption (2% SO_2/98% N_2); (**c**) [C_4mim][OAc] after CO_2 absorption (15% CO_2/85% N_2); (**d**) Fresh [NH_2emim][BF_4]; (**e**) [NH_2emim][BF_4] after SO_2 absorption (2% SO_2/98% N_2); (f) [NH_2emim][BF_4] after CO_2 absorption (15% CO_2/85% N_2).

In contrast, the chemical reaction between SO_2 and [C_4mim][OAc] was much stronger than that of [C_4mim][OAc]–CO_2. Even if there was only a small amount of SO_2 (2%) in the flue gas, the FT-IR spectrum still shows marked changes (Figure 3b). Compared with the spectrum of fresh [C_4mim][OAc], the peak intensity at 1580 and 1371 cm^{-1} decreased significantly as the [C_4mim][OAc] absorbing SO_2. Meanwhile, the peaks at 1720, 1321, 1254, 1144, and 950 cm^{-1} newly appeared in the spectrum.

The bands at 1321 and 1144 cm^{-1} can be attributed to the stretching of SO_2 absorbed by the ionic liquid [26]. After SO_2 absorption, the new peak at 1720 cm^{-1} shows the formation of a carbonyl group, which also indicates that most of the acetate ions were no longer associated with [C_4mim] cations. The intense band at 950 cm^{-1} should be assigned to the vibrational mode of SO_3^{2-} or $S_2O_5^{2-}$. It once again suggests that the interaction between the SO_2 and [C_4mim][OAc] ionic liquid was strong. Similarly, the peak intensity at 885 and 1543 cm^{-1} changed markedly when the [NH_2emim][BF_4] absorbed SO_2. Particularly, two new peaks appeared at 968 and1367 cm^{-1}, which can be attributed to the interaction between the N elements of the IL and SO_2 [6].

2.2. CO_2/SO_2 Absorption Properties in IL Mixtures

Due to the influence of SO_2, the CO_2 absorption capacity of single ionic liquids was greatly decreased. If [NH_2emim][BF_4] and [C_4mim][OAc] were simultaneously utilized, more CO_2 (with SO_2) in the flue gas might be captured. The CO_2 absorption capacities of IL mixtures at different mole fractions of [C_4mim][OAc] or [NH_2emim][BF_4] were displayed in Figure 4. Here, *X* is defined as the molar ratio of [NH_2emim][BF_4] to the IL mixture ([C_4mim][OAc]/[NH_2emim][BF_4]). Compared with the CO_2 absorption capacity of the single IL, the IL mixture could remove more CO_2. This result may be due to the presence of [NH_2emim][BF_4]. The small amount of SO_2 might be absorbed by [NH_2emim][BF_4] at first. Without the interference of SO_2, the CO_2 absorption capacity of the IL mixture was significantly enhanced. It was also found that the absorption of CO_2 did not increase significantly with the increase of the *X* value. When *X* was 0.3, the CO_2 absorption capacity of the [C_4mim][OAc]/[NH_2emim][BF_4] mixture reached up to the maximum. Similarly, when the IL mixture [C_4mim][OAc]/[NH_2emim][OAc] was used to remove CO_2/SO_2 of the flue gas, the poison effect of SO_2 on [C_4mim][OAc] was also greatly reduced. As Figure 4 shows, the CO_2 absorption of [C_4mim][OAc]/[NH_2emim][OAc] was about 0.4 mol CO_2/mol IL. Compared to the single [C_4mim][OAc], the absorption capacity of the IL mixture was improved.

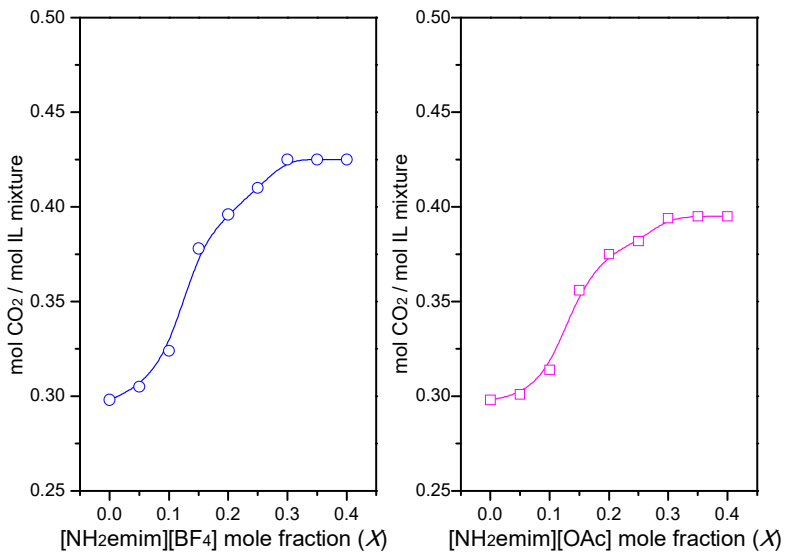

Figure 4. CO_2 absorption capacity of ionic liquid (IL) mixtures at different *X*: Flue atmosphere 15% CO_2/2% SO_2/83% N_2; absorption temperature, 293 K.

The ^{1}H NMR spectrum (Figure 5) shows that SO_2 would interact with [NH_2emim][BF_4] and [NH_2emim][OAc]. The NMR data of fresh [NH_2emim][BF_4] and fresh [NH_2emim][OAc] are listed as follows:

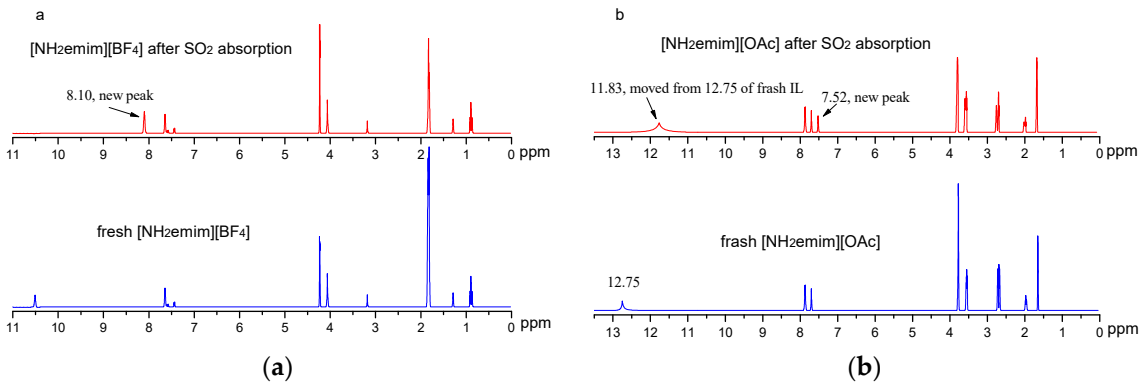

(**a**) (**b**)

Figure 5. ^{1}H NMR spectra of ILs: (**a**) [NH_2emim][BF_4]; (**b**) [NH_2emim][OAc].

Fresh [NH_2emim][BF_4], δ = 7.721 (s, 1H, unsaturated C−H in the imidazole ring, with N connected to the left and right), 7.641 (d, 1H, unsaturated C−H in the imidazole ring), 7.636 (d, 1H, unsaturated C−H in the imidazole ring), 4.295 (s, 3H, H_3C−N ring), 4.039 (t, 2H, H_2C−N ring), 3.112 (m, 2H, N−CH_2−C−N ring), and 1.878 (t, 2H, NH_2).

Fresh [NH_2emim][OAc], δ = 12.751 (s, 1H, unsaturated C−H in the imidazole ring, with N connected to the left and right), 7.865 (d, 1H, unsaturated C−H in the imidazole ring), 7.703 (d, 1H, unsaturated C−H in the imidazole ring), 3.577 (s, 3H, H_3C−N ring), 3.749 (t, 2H, H_2C−N ring), 2.693 (m, 2H, N−CH_2−C−N ring), 1.973 (t, 2H, NH_2) and 1.651 (s, 3H, CH_3 in OAc-).

In comparison to the ^{1}H NMR spectrum of the fresh [NH_2emim][BF_4] (Figure 5a), new resonance peaks at 8.10 ppm were found after SO_2 absorption, which indicates the formation of S⋯N [28]. According to this result, it was considered that the interaction between SO_2 and [NH_2emim][BF_4] should mainly occur at the N element of the [NH_2emim] cation. For the case of the [NH_2emim][OAc] (Figure 5b), a typical peak of −COOH in the ^{1}H NMR spectrum moved from 12.75 to 11.83 ppm, and a new resonance peak was observed at 7.52 ppm after SO_2 absorption. These results suggest that the interaction between [NH_2emim][OAc] and SO_2 had occurred [25]. That is, the interaction between [OAc] and SO_2 leads to the moving from 12.75 ppm to 11.83, while the reaction of [NH_2emim] and SO_2 makes the new peak 7.52 ppm appearance.

In order to further investigate the effects of SO_2 on the CO_2 absorption capacity of ionic liquids, the CO_2 absorption performance of fresh IL and after SO_2-saturated IL are illustrated in Figure 6. Specifically, fresh [C_4mim][OAc] and fresh [NH_2emim][BF_4] ionic liquids were used to absorb SO_2 at first. When the IL was saturated by SO_2, the CO_2 absorption performance of the IL was investigated. It was found that the SO_2-saturated [C_4mim][OAc] did not have the ability to absorb CO_2. The concentration of CO_2 at the outlet was almost equal to that at the inlet. While fresh [C_4mim][OAc] can absorb CO_2 even after 60 min. The similar results were also observed using fresh [C_2mim][OAc] and SO_2 saturated [C_2mim][OAc] to absorb CO_2 [24]. Shiflet et al. considered that the interaction between the [OAc] anion and CO_2 plays an important role in the CO_2 removal of [OAc]−based ionic liquids [8]. However, the presence of SO_2 makes a great impact on the CO_2 absorption of [C_4mim][OAc]. In contrast, when [NH_2emim][BF_4] was saturated by SO_2, the [NH_2emim][BF_4] still had the CO_2 absorption capacity. As Figure 6b shows, SO_2-saturated [NH_2emim][BF_4] could capture about 2−7% CO_2 during the absorption process.

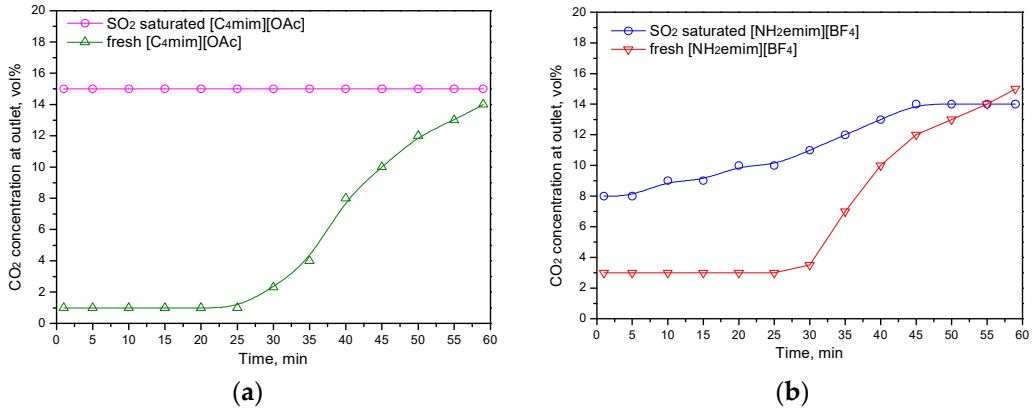

Figure 6. CO_2 absorption performance of fresh IL and after SO_2 saturated IL: (**a**) [C_4mim][OAc]; (**b**) [NH_2emim][BF_4].

2.3. Quantum Chemical Calculation on the Interaction of IL Mixture with CO_2/SO_2

The absorption capacity of CO_2 in the IL mixtures was higher than that of the single ionic liquid. This may be related to the interactions between ILs and CO_2/SO_2 molecules. Thus, the interaction of the [C_4mim][OAc] anion and [NH_2emim][BF_4] with CO_2/SO_2 was deeply investigated through quantum chemical calculation, which might be helpful to understand well the roles of CO_2 and SO_2 in the IL absorption. In this work, the structure of [NH_2emim][BF_4] and [C_4mim][OAc] was optimized on the basis of DFT-D3 calculation at first. The configuration of the IL with the lowest energy was considered as the optimized structure. Additionally, the structures of [C_4mim][OAc] and [NH_2emim][BF_4] with CO_2 and SO_2 were also investigated (Figure 7). The structural parameters for the IL−CO_2/SO_2 complexes are listed in Table 2.

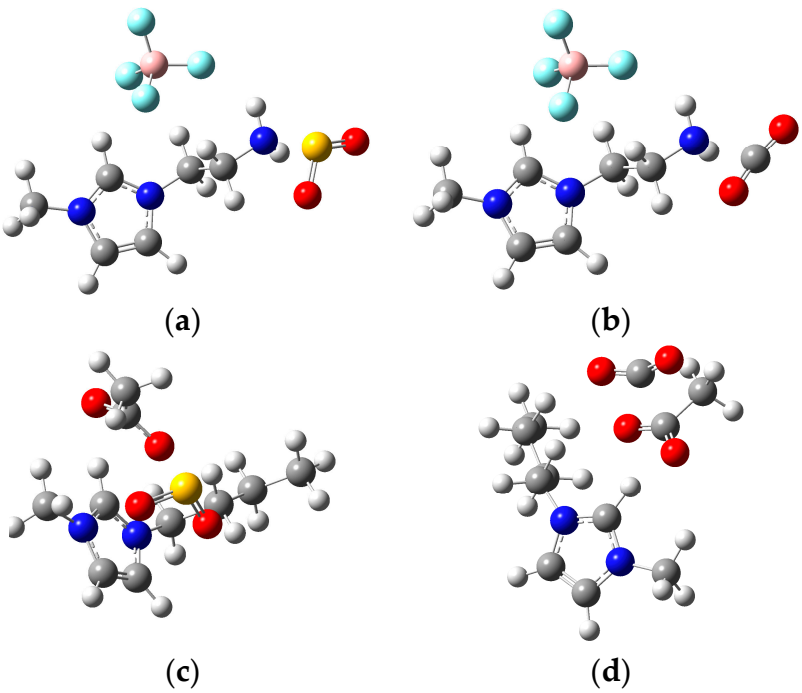

Figure 7. Optimized structure of the complexes of IL with CO_2/SO_2: (**a**) [NH_2emim][BF_4]−SO_2; (**b**) [NH_2emim][BF_4]−CO_2; (**c**) [C_4mim][OAc]−SO_2; (**d**) [C_4mim][OAc]−CO_2.

Table 2. Structural parameters for the complexes.

Structural Parameters	CO_2−[NH_2emim][BF_4]	SO_2−[NH_2emim][BF_4]	[C_4mim][OAc]−CO_2	[C_4mim][OAc]−SO_2
C−O, Å	1.19		1.21	
∠O−C−O, °	166		146	
S−O, Å		1.46		1.49
∠O−S−O, °		113.5		112.6

In general, the CO_2/SO_2 gas molecules around the anions and cations were related to the absorption reaction. As Figure 7a shows, there was a strong interaction between the N atom and the S atom of SO_2. Due to the complexation of $SO_2 \cdots$ N, the average angle of SO_2 was 116.0°. Compared to 119.5° of the pure SO_2 molecule, the bending degree of O=S=O was increased. Similarly, [NH_2emim][BF_4] also leads to an impact on the CO_2 structure. The angle of CO_2 was bent from 180° to 166°, and the bond length of C−O was extended from 1.16 Å to 1.19 Å. For the cases of [C_4mim][OAc], the interaction between the O and the C atom of carbon dioxide was also strong due to the negatively charged oxygen (O atom) in the [OAc] anion. The curvature of CO_2 could be increased by the interaction of the [OAc] anion. The average angle of CO_2 was bent to 146°, and the bond length of C−O was elongated to 1.21 Å. The configurations in Figure 7 also suggest that [NH_2emim] cation and [OAc] anion are the active sites for CO_2/SO_2 absorption.

To some extent, the interaction energy and absorption enthalpy might reflect the absorption capacity of the ILs. It was found that the NH_2emim] cation and [OAc] anion were the main active sites for the absorption of CO_2 and SO_2. In order to save the calculation cost and reduce the interference of other ions, herein, only the thermodynamic data of [OAc]−CO_2, [OAc]−SO_2, CO_2−[NH_2emim], and SO_2−[NH_2emim] complexes were compared (Table 3). It was found that the interaction energy and absorption enthalpy of [OAc]−CO_2−SO_2 complex were less than the sum of the energy and the enthalpy for [OAc]−CO_2 and [OAc]−SO_2, suggesting that CO_2 and SO_2 would competitively react with [OAc] anion.

Table 3. Thermochemical parameters and charge transfer of the ion−CO_2/SO_2 complexes.

	OAc−CO_2	OAc−SO_2	OAc−CO_2−SO_2
ΔE, kJ/mol	−40.7	−113.4	−140.0
ΔH, kJ/mol	−46.5	−125.1	−151.4
ΔG, kJ/mol	−1.6	−70.8	−72.1
net charge transfer, e	−0.510	−0.382	−0.035(CO_2)/−0.316(SO_2)
	CO_2−[NH_2emim]	**SO_2−[NH_2emim]**	**SO_2−CO_2−[NH_2emim]**
ΔE, kJ/mol	−33.8	−123.9	−156.8
ΔH, kJ/mol	−36.3	−126.7	−160.1
ΔG, kJ/mol	−7.2	−55.1	−61.9
net charge transfer, e	−0.312	−0.399	−0.308(CO_2)/−0.334(SO_2)

In contrast, the interaction energy and absorption enthalpy of [NH_2emim]−CO_2−SO_2 complex were approximately equal to the sum of those for the [NH_2emim]−CO_2 and [NH_2emim]−SO_2 complexes, indicating that the competitive reaction between [NH_2emim]−CO_2 and [NH_2emim]−SO_2 was not obvious. The absorption reaction might also lead to a change in charge distribution. It was found that the amount of net charge transfer from CO_2 to [NH_2emim] in [NH_2emim]−CO_2−SO_2 complex was almost equal to that of [NH_2emim]−CO_2, suggesting that [NH_2emim] had strong interactions with either SO_2 or CO_2. However, due to the impact of SO_2, the net charge transfer from [OAc] to CO_2 was significantly reduced from −0.510 in the [OAc]−CO_2 complex to −0.035 in [OAc]−CO_2−SO_2 complex, respectively, which might account for the decrease of CO_2 absorption capacity for [C_4mim][OAc] in Table 1.

Table 4 collects the thermochemical data of $[NH_2emim][BF_4]-CO_2$ and $[NH_2emim][BF_4]-SO_2$ complexes. In order to consider the solvent effect of ionic liquids, the continuum universal solvation model (SMD) was used in the calculation. Based on the SMD model, the interaction energies of $[NH_2emim][BF_4]-CO_2$ and $[NH_2emim][BF_4]-SO_2$ system were −16.8 and −76.3 kJ/mol, respectively. They were lower than those in the gas phase (−19.2 and −85.4 kJ/mol). Notably, the difference between the interaction energy ($[NH_2emim][BF_4]-CO_2$ and $[NH_2emim][BF_4]-SO_2$) in the gas phase (59.5 kJ/mol) was very consistent with the energy difference (66.2 kJ/mol) using the SMD model. In the liquid phase, the interaction energy between $[NH_2emim][BF_4]$ and SO_2 was slightly greater than that of $[NH_2emim][BF_4]-CO_2$, suggesting that $[NH_2emim][BF_4]$ tends to react with SO_2 rather than with CO_2 during the absorption process. Similarly, this phenomenon could also be observed in the thermodynamic data of the $[C_4mim][OAc]-CO_2$ and $[C_4mim][OAc]-SO_2$ complexes. In short, SO_2 was more active than CO_2 in the reaction with ionic liquids, and the $[NH_2emim][BF_4]$ may be more likely to absorb SO_2.

Table 4. Thermochemical parameters for the IL−CO_2/SO_2 complexes [a].

	$[C_4mim][OAc]-CO_2$	$[C_4mim][OAc]-SO_2$	$CO_2-[NH_2emim][BF_4]$	$SO_2-[NH_2emim][BF_4]$
ΔE, kJ/mol	−26.4 (−21.9)	−80.1 (−70.5)	−19.2 (−16.8)	−85.4 (−76.3)
ΔH, kJ/mol	−30.5	−93.2	−29.1	−91.5
ΔG, kJ/mol	−2.7	−40.6	8.1	−37.2

[a] Values of brackets were calculated by the continuum universal solvation model (SMD).

The interaction between IL mixture ($[C_4mim][OAc]/[NH_2emim][BF_4]$) and CO_2/SO_2 has also been investigated by the quantum chemistry calculation. The optimized structure is displayed in Figure 8. In the mixed ionic liquids, it is found that SO_2 was close to $[NH_2emim][BF_4]$, while the CO_2 molecule was near the $[C_4mim][OAc]$ ionic liquid. Specifically, SO_2 would have interacted with the N atom on the $[NH_2emim]$ cation, and CO_2 was more likely to react with the [OAc] anion. This result might explain why the IL mixture can more effectively absorb the CO_2 of flue gas. Because of the existence of $[NH_2emim][BF_4]$, SO_2 may be first captured by $[NH_2emim]$. Without the interference of SO_2, the $[C_4mim][OAc]$ ionic liquid then could absorb more CO_2.

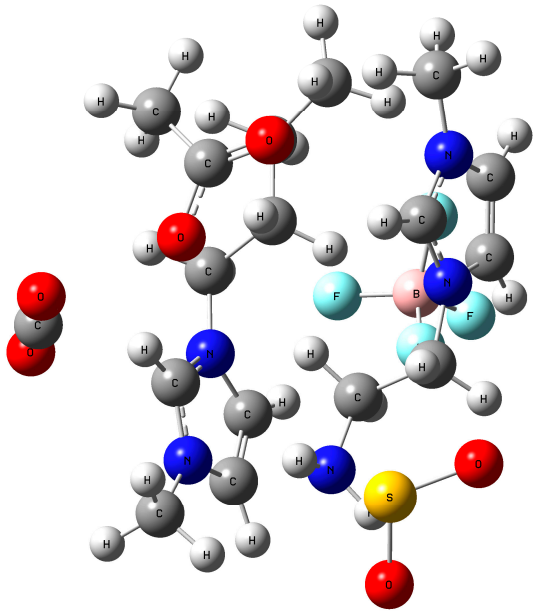

Figure 8. Optimized structure of the IL mixture and CO_2/SO_2.

3. Materials and Methods

3.1. Materials

The simulated flue gas was obtained by pure gas CO_2, SO_2, and N_2 (purity of >99.99 wt%). They were all purchased from Beifen (China) Gas Technology Company. 1-butyl-3-methylimidazolium tetrafluoroborate ([C_4mim][BF_4], 99 wt%) was obtained from Sigma-Aldrich Chemical Co., but the ionic liquid 1-butyl-3-methylimidazolium acetate ([C_4mim][OAc], 99 wt%) were purchased from Lanzhou Greenchem ILs, LICP, CAS, China. Additionally, [NH_2emim][BF_4] and [NH_2emim][OAc] have been synthesized by ourselves in this work. The used materials were as follows: 1-methylimidazole ($C_4H_6N_2$), 2-bromoethylamine hydrobromide ($C_2H_7Br_2N$), sodium acetate anhydrous (CH_3COONa), 1-methylimidazole ($C_4H_6N_2$), acetic acid (CH_3COOH), and sodium borate ($NaBF_4$). They were all provided by Sinopharm Chemical Reagent Co., Ltd., China, with purity over 98 wt%.

3.2. Ionic Liquid Preparation

In this work, the ionic liquids [NH_2emim][BF_4] and [NH_2emim][OAc] were prepared by ourselves according to the method used in the literature [17,18,29]. First, the [NH_2emim] cation was prepared by the reaction of 1-methylimidazole and 2-bromoethylamine hydrobromide under reflux for 12 h. Second, the [NH_2emim]-based IL was simply synthesized by ion exchange with $NaBF_4$ or NaOAc/CH_3COOH in ethanol, and then the ethanol was removed in vacuum. The structures of the ILs were confirmed by proton nuclear magnetic resonance (^{1}H NMR, Bruker WB400 AMX spectrometer, Billerica, MA, USA). Here, deuterated chloroform ($CDCl_3$) was used as a solvent, and tetramethylsilane (TMS) was employed as an internal standard for ^{1}H NMR measurement.

3.3. CO_2 and SO_2 Absorption

As Figure 9 shows, CO_2 and SO_2 absorption experiments were performed in a 30 mL reactor immersed with a water-bath temperature controller. The temperatures were controlled at 293 K for absorption and 353 K for desorption, respectively. The simulated flue gas was a mixture of N_2, CO_2, and SO_2 in accordance with a certain proportion. As a typical absorption process, 10 mL IL or IL mixtures were added to the reactor at first. Subsequently, 15 vol% CO_2, 2 vol% SO_2 and 83 vol% N_2 were mixed in storage. The intake speed of the mixed gas was controlled at 60 mL/min, and the absorption pressure was controlled at 101.3 kPa. The concentrations of CO_2 and SO_2 were analyzed by a gas analyzer (MRU NOVA2000) at the outlet. To investigate the IL regeneration, CO_2 or SO_2 saturated IL was also loaded in the reactor. Desorption was performed at 353 K under a pure N_2 gas atmosphere for 30 min.

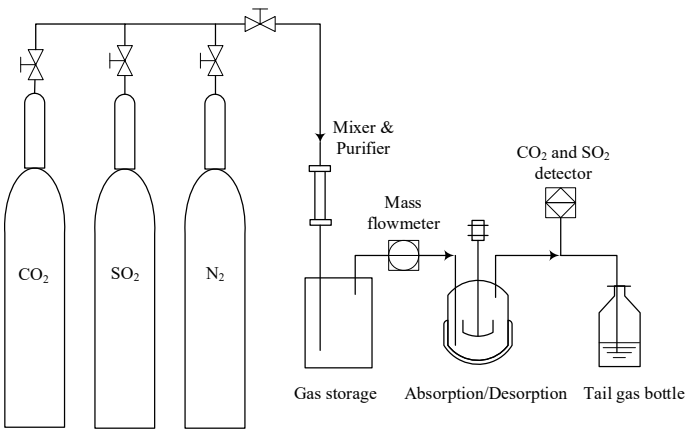

Figure 9. Schematic diagram of the apparatus used for absorption and desorption.

The amount of absorbed CO_2 or SO_2 was calculated by the following equation.

$$A_{gas} = \frac{M_{IL}\rho_{gas}Q\int_{t_1}^{t_2}(C_0 - C_{gas}(t))\mathrm{d}t}{m_{IL}M_{gas}}$$

where A_{gas} is the molar amount of CO_2 or SO_2 in the ionic liquid; Q is the flow rate of the gas stream; C_0 and C_{gas} are the CO_2 or SO_2 concentrations at the inlet and the outlet streams, respectively; t_1 refers to the beginning time of the absorption process; when the CO_2 and SO_2 concentration at the outlet stream returns to the initial concentration, the time is t_2; M_{IL} and M_{gas} are the molecular weight of IL and CO_2 (or SO_2), respectively; m_{IL} is the weight of the ILs, and ρ_{gas} is the density of CO_2 or SO_2.

After the IL was saturated by CO_2 and SO_2, the complex structure was investigated by the FTIR and NMR technologies. The FTIR spectra of the samples were analyzed on an FTIR spectrometer (PerkinElmer, Frontier 2500). In addition, the structure changes of the [NH_2emim]-based IL after absorption were also detected by the NMR spectrometer (Bruker WB400 AMX, 300 MHz) using chloroform-*d* ($CDCl_3$) as a solvent and tetramethylsilane (TMS) as an internal standard.

3.4. Theoretical Calculation

A quantum chemical calculation was used in this work to study the interaction between the ionic liquid and CO_2 with SO_2. All calculations were carried out by the Gaussian 16 program [30]. For IL calculations, Li et al. [31] suggested that the density function of the Minnesota family [32] (e.g., M06-2X) with a diffusion function basis set (e.g., 6-311++G(d,p)) might give reasonable results. If dispersion-corrected density functionals (e.g., gd3bj, DFT-D3) were used, more reliable results could be obtained [33]. Therefore, the geometry optimization and frequency analysis of all ILs and IL mixtures were performed at the M06-2X/6-311++G(d,p) level and correction with Grimme's method. In order to calculate the interaction energy of the IL complexes, the basis set superposition error (BSSE) method was employed to correct the energy results [34]. The effect of the solvent should be taken into consideration in the theoretical calculation of the ionic liquids. It was found that the SMD solvation model proposed by Truhlar et al. can be used for the IL calculation very well [35,36]. Thus, the density functional theory (M06-2X and dispersion-corrected method) with the SMD model was also used to calculate the interaction energy of IL−CO_2/SO_2.

4. Conclusions

The CO_2 and SO_2 absorption of the flue gas in ionic liquids were investigated by the experimental method and theoretical calculation. The single ionic liquids, such as [NH_2emim][BF_4] and [C_4mim][OAc], all showed good CO_2 absorption performance for the simulated flue gas without SO_2 interference. However, SO_2 was more likely to react with the active sites of the ILs. When SO_2 was in the flue gas, the CO_2 absorption capacity of the single ionic liquid would be significantly inhibited. It was found that the interference of SO_2 on the CO_2 absorption performance might be markedly reduced by using the ionic liquid mixtures. The CO_2 absorption capacity of the IL mixture [C_4mim][OAc]/[NH_2emim][BF_4] was about 0.4 mol CO_2/mol IL even at an atmosphere of 15% CO_2/2%SO_2/83% N_2, which was greater than that of single [C_4mim][OAc] (0.204 mol CO_2/mol IL). There was a competitive relationship between CO_2 and SO_2 during the absorption process. The single ILs prefer to capture SO_2 rather than remove CO_2, due to the stronger interaction energy of SO_2 and the ILs. The experimental and calculated results suggested that the [OAc] anion and [NH_2emim] cation are the main active sites for CO_2 and SO_2 absorption. A lower absorption enthalpy of the IL−SO_2 or IL−CO_2 system usually means low absorption capacity. Thus, for the IL mixture [C_4mim][OAc]/[NH_2emim][BF_4], the quantum calculation results indicated that [NH_2emim][BF_4] might be more likely to absorb SO_2 of the flue gas and CO_2 was easily removed by the [C_4mim][OAc].

Author Contributions: Funding acquisition, Y.L.; investigation, G.W., Y.L., and G.L.; methodology, Y.L.; data curation, X.P.; writing—original draft, G.W., and Y.L. All authors have read and agreed to the published version of the manuscript.

Funding: This research and the APC were funded by the National Natural Science Foundation of China (grant numbers: 21766021 and 21266015).

Conflicts of Interest: The authors declare no conflict of interest.

References

1. Aghaie, M.; Rezaei, N.; Zendehboudi, S. A systematic review on CO_2 capture with ionic liquids: Current status and future prospects. *Renew. Sustain. Energy Rev.* **2018**, *96*, 502–525. [CrossRef]
2. Yu, C.H.; Huang, C.H.; Tan, C.S. A review of CO_2 capture by absorption and adsorption. *Aerosol Air Qual. Res.* **2012**, *12*, 745–769. [CrossRef]
3. Wang, B.; Qin, L.; Mu, T.; Xue, Z.; Gao, G. Are ionic liquids chemically stable? *Chem. Rev.* **2017**, *117*, 7113–7131. [CrossRef]
4. Zhang, S.; Sun, N.; He, X.; Lu, X.; Zhang, X. Physical properties of ionic liquids: Database and evaluation. *J. Phys. Chem. Ref. Data* **2006**, *35*, 1475–1517. [CrossRef]
5. Blanchard, L.A.; Hancu, D.; Beckman, E.J.; Brennecke, J.F. Green processing using ionic liquids and CO_2. *Nature* **1999**, *399*, 28–29. [CrossRef]
6. Wang, C.M.; Cui, G.K.; Luo, X.Y.; Xu, Y.J.; Li, H.R.; Dai, S. Highly efficient and reversible SO_2 capture by tunable azole-based ionic liquids through multiple-site chemical absorption. *J. Am. Chem. Soc.* **2011**, *133*, 11916–11919. [CrossRef]
7. Shiflett, M.B.; Yokozeki, A. Separation of carbon dioxide and sulfur dioxide using room-temperature ionic liquid [bmim][MeSO4]. *Energy Fuels* **2010**, *24*, 1001–1008. [CrossRef]
8. Shiflett, M.B.; Yokozeki, A. Solubilities and diffusivities of carbon dioxide in ionic liquids: Bmim PF_6 and bmim BF_4. *Ind. Eng. Chem. Res.* **2005**, *44*, 4453–4464. [CrossRef]
9. Zhang, X.; Jiang, K.; Liu, Z.; Yao, X.; Liu, X.; Zeng, S.; Dong, K.; Zhang, S. Insight into the performance of acid gas in ionic liquids by molecular simulation. *Ind. Eng. Chem. Res.* **2019**, *58*, 1443–1453. [CrossRef]
10. Shang, Y.; Li, H.P.; Zhang, S.J.; Xu, H.; Wang, Z.X.; Zhang, L.; Zhang, J.M. Guanidinium-based ionic liquids for sulfur dioxide sorption. *Chem. Eng. J.* **2011**, *175*, 324–329. [CrossRef]
11. Izgorodina, E.I.; Hodgson, J.L.; Weis, D.C.; Pas, S.J.; MacFarlane, D.R. Physical absorption of CO_2 in protic and aprotic ionic liquids: An interaction perspective. *J. Phys. Chem. B* **2015**, *119*, 11748–11759. [CrossRef] [PubMed]
12. Karousos, D.S.; Kouvelos, E.; Sapalidis, A.; Pohako-Esko, K.; Bahlmann, M.; Schulz, P.S.; Wasserscheid, P.; Siranidi, E.; Vangeli, O.; Falaras, P.; et al. Novel inverse supported ionic liquid absorbents for acidic gas removal from flue gas. *Ind. Eng. Chem. Res.* **2016**, *55*, 5748–5762. [CrossRef]
13. Li, X.S.; Zhang, L.Q.; Zheng, Y.; Zheng, C.G. Effect of SO_2 on CO_2 absorption in flue gas by ionic liquid 1-ethyl-3-methylimidazolium acetate. *Ind. Eng. Chem. Res.* **2015**, *54*, 8569–8578. [CrossRef]
14. Wang, C.; Luo, X.; Luo, H.; Jiang, D.E.; Li, H.; Dai, S. Tuning the basicity of ionic liquids for equimolar CO_2 capture. *Angew. Chem. Int. Ed.* **2011**, *50*, 4918–4922. [CrossRef] [PubMed]
15. Lei, Z.G.; Dai, C.N.; Chen, B.H. Gas solubility in ionic liquids. *Chem. Rev.* **2014**, *114*, 1289–1326. [CrossRef] [PubMed]
16. Goodrich, B.F.; de la Fuente, J.C.; Gurkan, B.E.; Zadigian, D.J.; Price, E.A.; Huang, Y.; Brennecke, J.F. Experimental measurements of amine-functionalized anion-tethered ionic liquids with carbon dioxide. *Ind. Eng. Chem. Res.* **2011**, *50*, 111–118. [CrossRef]
17. Bates, E.D.; Mayton, R.D.; Ntai, I.; Davis, J.H. CO_2 capture by a task-specific ionic liquid. *J. Am. Chem. Soc.* **2002**, *124*, 926–927. [CrossRef]
18. Wang, M.; Zhang, L.Q.; Gao, L.X.; Pi, K.W.; Zhang, J.Y.; Zheng, C.G. Improvement of the CO_2 absorption performance using ionic liquid [NH_2emim][BF_4] and [Emim][BF_4]/[Bmim][BF_4] mixtures. *Energy Fuels* **2013**, *27*, 461–466. [CrossRef]
19. Damas, G.B.; Dias, A.B.A.; Costa, L.T. A quantum chemistry study for ionic liquids applied to gas capture and separation. *J. Phys. Chem. B* **2014**, *118*, 9046–9064. [CrossRef]
20. Amarasekara, A.S. Acidic Ionic Liquids. *Chem. Rev.* **2016**, *116*, 6133–6183. [CrossRef]

21. Rezaei, F.; Jones, C.W. Stability of supported amine adsorbents to SO_2 and NO_x in postcombustion CO_2 capture. 1. Single-component adsorption. *Ind. Eng. Chem. Res.* **2013**, *52*, 12192–12201. [CrossRef]
22. Hallenbeck, A.P.; Kitchin, J.R. Effects of O_2 and SO_2 on the capture capacity of a primary-amine based polymeric CO_2 sorbent. *Ind. Eng. Chem. Res.* **2013**, *52*, 10788–10794. [CrossRef]
23. Shiflett, M.B.; Yokozeki, A. Chemical absorption of sulfur dioxide in room-temperature ionic liquids. *Ind. Eng. Chem. Res.* **2010**, *49*, 1370–1377. [CrossRef]
24. Shiflett, M.B.; Drew, D.W.; Cantini, R.A.; Yokozeki, A. Carbon dioxide capture using ionic liquid 1-butyl-3-methylimidazolium acetate. *Energy Fuels* **2010**, *24*, 5781–5789. [CrossRef]
25. Li, W.; Liu, Y.; Wang, L.; Gao, G. Using ionic liquid mixtures to improve the so_2 absorption performance in flue gas. *Energy Fuels* **2017**, *31*, 1771–1777. [CrossRef]
26. Lee, K.Y.; Kim, H.S.; Kim, C.S.; Jung, K.D. Behaviors of SO_2 absorption in BMIm OAc as an absorbent to recover SO_2 in thermochemical processes to produce hydrogen. *Int. J. Hydrog. Energy* **2010**, *35*, 10173–10178. [CrossRef]
27. Gurau, G.; Rodríguez, H.; Kelley, S.P.; Janiczek, P.; Kalb, R.S.; Rogers, R.D. Demonstration of chemisorption of carbon dioxide in 1,3-dialkylimidazolium acetate ionic liquids. *Angew. Chem. Int. Ed.* **2011**, *50*, 12024–12026. [CrossRef] [PubMed]
28. Zhai, L.Z.; Zhong, Q.; He, C.; Wang, J. Hydroxyl ammonium ionic liquids synthesized by water-bath microwave: Synthesis and desulfurization. *J. Hazard. Mater.* **2010**, *177*, 807–813. [CrossRef]
29. Kurnia, K.A.; Mutalib, M.I.A.; Ariwahjoedi, B. Estimation of physicochemical properties of ionic liquids $[H_2N\text{-}C_2mim][BF_4]$ and $[H_2N\text{-}C_3mim][BF_4]$. *J. Chem. Eng. Data* **2011**, *56*, 2557–2562. [CrossRef]
30. Frisch, M.J.; Trucks, G.W.; Schlegel, H.B.; Scuseria, G.E.; Robb, M.A.; Cheeseman, J.R.; Scalmani, G.; Barone, V.; Mennucci, B.; Petersson, G.A.; et al. *Gaussian 16 (Revision A.01)*; Gaussian, Inc.: Wallingford, CT, USA, 2016.
31. Li, H.P.; Chang, Y.H.; Zhu, W.S.; Jiang, W.; Zhang, M.; Xia, J.X.; Yin, S.; Li, H.M. A DFT Study of the Extractive Desulfurization Mechanism by BMIM (+) AlCl4 (-) Ionic Liquid. *J. Phys. Chem. B* **2015**, *119*, 5995–6009. [CrossRef]
32. Zhao, Y.; Truhlar, D.G. A new local density functional for main-group thermochemistry, transition metal bonding, thermochemical kinetics, and noncovalent interactions. *J. Chem. Phys.* **2006**, *125*, 194101–194118. [CrossRef] [PubMed]
33. Grimme, S.; Hujo, W.; Kirchner, B. Performance of dispersion-corrected density functional theory for the interactions in ionic liquids. *Phys. Chem. Chem. Phys.* **2012**, *14*, 4875–4883. [CrossRef] [PubMed]
34. Boys, S.F.; Bernardi, F. The Calculations of Small Molecular Interaction by the Difference of Separate Total Energies. Some Procedures with Reduced Error. *Mol. Phys.* **1970**, *19*, 553–566. [CrossRef]
35. Bernales, V.S.; Marenich, A.V.; Contreras, R.; Cramer, C.J.; Truhlar, D.G. Quantum Mechanical Continuum Solvation Models for Ionic Liquids. *J. Phys. Chem. B* **2012**, *116*, 9122–9129. [CrossRef] [PubMed]
36. Marenich, A.V.; Cramer, C.J.; Truhlar, D.G. Universal solvation model based on solute electron density and on a continuum model of the solvent defined by the bulk dielectric constant and atomic surface tensions. *J. Phys. Chem. B* **2009**, *113*, 6378–6396. [CrossRef]

Sample Availability: Samples of the ionic liquids are available from the authors.